

Spectroscopy of ^{146}Sm via the (d, t) and of ^{148}Sm via the (d, t) and (d, p) reactions*

W. Oelert, J. V. Maher, D. A. Sink, and M. J. Spisak

Nuclear Physics Laboratory, University of Pittsburgh, Pittsburgh, Pennsylvania 15260

(Received 3 April 1975)

The (d, t) reaction on the isotopes ^{147}Sm and ^{149}Sm has been investigated at a deuteron energy of 17 MeV; the (d, p) reaction on the isotope ^{147}Sm at a deuteron energy of 12.5 MeV. Angular distributions were taken in 2.5° steps in the range of $7.5 \leq \theta_{\text{lab}} \leq 35^\circ$ and in 5° steps for $\theta_{\text{lab}} > 35^\circ$. The experimental energy resolution is 9–11 keV for the pickup reactions and 10–12 keV for the stripping case. Spectroscopic factors and l transfers were extracted by distorted wave Born approximation analysis. Eighty-three states in ^{146}Sm are observed; l transfer and J^π limits are given for 36 of them. For the nucleus ^{148}Sm 97 states are observed; l transfers and J^π limits are given for 63 of them. Reasonable $l = 3$, $l = 1$, and $l = 0$ summed strengths have been found. Comparison with (p, t) and (t, p) studies of the same final nuclei investigated here is made in a phenomenological collective picture.

[NUCLEAR REACTIONS $^{147}\text{Sm}(d, t)$ and $^{149}\text{Sm}(d, t)$, $E_d = 17$ MeV. $^{147}\text{Sm}(d, p)$,
 $E_d = 12.5$ MeV. Measured $\sigma(E_t, \theta)$, $\sigma(E_p, \theta)$; $^{146, 148}\text{Sm}$ level energies, resolution 9–12 keV, enriched targets, DWBA analysis.]

I. INTRODUCTION

The β and γ decay of rare earth isotopes have been extensively studied.^{1–5} However in the last few years one- and two-nucleon transfer studies have been of particular interest in this mass region.⁶ Among the deformed isotopes, qualitative agreement between spectroscopic factors extracted from distorted wave Born approximation (DWBA) analyses and Nilsson model calculations was obtained. While many transitions in the one-nucleon transfer reactions can be considered to proceed via a direct mechanism, a significant number of anomalous angular distributions have been observed in both (p, d) and (d, t) studies.⁷ There has been at least some success in explaining these anomalous angular distributions as arising from multistep processes.

The two-nucleon transfer studies undertaken in the rare earth region have been perhaps of more spectacular interest. A series of (p, t) and (t, p) studies have shown a strong population of excited 0^+ states in a variety of residual nuclei.^{8–10} Such transitions in the mass region $140 \leq A \leq 165$ have been explained by invoking a number of mechanisms including multistep processes and structure effects such as shell closures for the spherical nuclei, β vibrations for static deformed nuclei and shape coexistence arguments in the transition region. Pairing vibrational and quadrupole pairing vibrational considerations could explain several 0^+ and 2^+ states, populated with characteristically different yield in the two-neutron stripping or pickup case. However, detailed analysis of all the measured angular distributions has suffered from the

lack of microscopic model wave functions for the rare earth nuclei. Most of the single nucleon transfer information previously available in the shape transition region arose from data which did not include complete angular distributions. The aim of our work is a systematic investigation of this region using different reactions and energies as tools to study the relevant properties. Particularly in the paper presented here we investigate the question of overlap between low lying residual nuclear states and the target ground state by measuring the (d, t) reaction on the Sm isotopes 147 and 149 and the (d, p) reaction on ^{147}Sm . Unfortunately it is difficult to extract spectroscopic information from single nucleon transfer reactions on odd mass targets. For this reason such reactions have been largely neglected. However, we wish here to study the single particle/hole character of the interesting levels reported in two-neutron transfer investigations so the one-neutron transfer on these high spin ($\frac{7}{2}$) targets becomes more interesting.

II. EXPERIMENTAL PROCEDURE

The one-nucleon transfer reactions presented here were performed with the deuteron beam from the University of Pittsburgh three stage Van de Graaff accelerator. Because of the positive Q value of the (d, p) reaction ($Q = +5.918$ MeV) we used a 12.5 MeV deuteron beam in the stripping case in order to get reasonable energy resolution (by doing this we significantly sacrificed sensitivity of experimental angular distribution shape to orbital angular momentum transfer l). The beam was focused through a 1 mm wide by 2 mm high collima-

tor aperture, which was followed by an antiscatterer slit. The maximum angular divergence of the incident beam was less than 1° . The incident beam was continuously monitored by two NaI(Tl) scintillators at an angle of $\pm 38.8^\circ$ relative to the beam direction. Deuterons elastically scattered into these counters, as well as the charge collected in the Faraday cup, were used to normalize the relative differential cross sections at the various angles.

The ^{147}Sm and ^{149}Sm targets consisted of approximately $50 \mu\text{g}/\text{cm}^2$ of isotopically enriched Sm_2O_3 evaporated onto a $20\text{--}30 \mu\text{g}/\text{cm}^2$ carbon backings. The enrichment in both cases was better than $(97.8 \pm 0.1)\%$. Triton and proton reaction products were detected in $50 \mu\text{m}$ Kodak NTB nuclear emulsions in the focal plane of an Enge split-pole spectrograph used with an acceptance aperture of 1.3 msr. The exposed plates were scanned at the Argonne National Laboratory automatic scanner¹¹ as well as by hand.

Figure 1 shows typical energy spectra for the reactions $^{147}\text{Sm}(d,t)^{146}\text{Sm}$, $^{149}\text{Sm}(d,t)^{148}\text{Sm}$, and $^{147}\text{Sm}(d,p)^{148}\text{Sm}$. The peak fitting program AUTO-FIT¹² was employed to analyze the energy spectra; numerous checks by hand were made to ensure the reliability of the fitting procedure, especially in the regions of high level density. Differential cross sections were measured at 2.5° intervals from 7.5 to 35° laboratory angle and then in 5° intervals to 80° [in the case of $^{149}\text{Sm}(d,t)$ to 65°]. The data were analyzed up to ~ 4 MeV excitation energy for the (d,t) reactions and up to 3.5 MeV in the case of the (d,p) reaction. Reliable excitation energies could be extracted and are summarized in the tables below, the values given are believed to be accurate to $\pm 0.1\%$ or 3 keV whichever is larger.

In addition to the random errors shown in the angular distributions below, which are due to counting statistics and background uncertainties alone, some further likely errors ought to be mentioned: (a) A scale error of up to 15% due to uncertainty of the target thickness and uniformity cannot be excluded when absolute cross sections are determined by the charge integration method. We have also determined absolute cross sections by normalizing the yield of elastically scattered deuterons measured in the 38.8° monitor detectors to the elastic scattering cross section expected on the basis of optical model calculations with the parameters discussed below. (b) Because the collimators which determine the spectrograph entrance aperture are continuously variable, uncertainty in reproducing collimator settings introduces a small error ($< 10\%$) in absolute solid angle and thus in absolute cross section. (c) By comparing results from the two methods of plate scanning a random

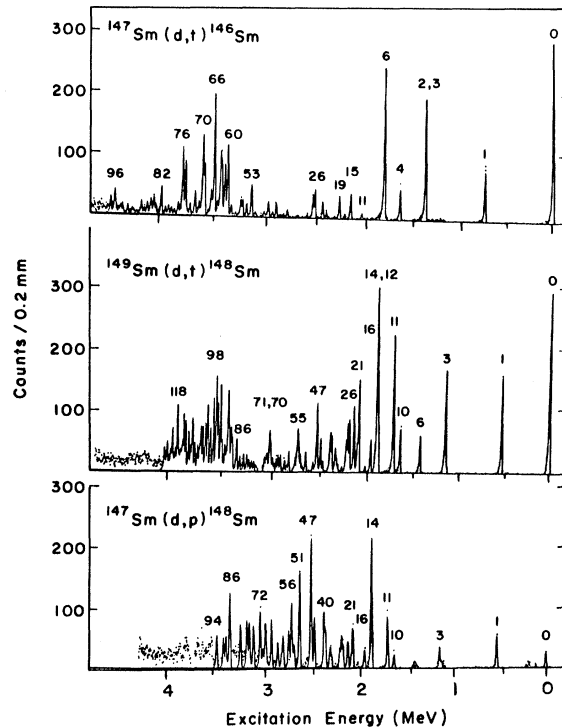


FIG. 1. Energy spectra for the reactions $^{147}\text{Sm}(d,t)$, $^{149}\text{Sm}(d,t)$, and $^{147}\text{Sm}(d,p)$ all at $\theta_{\text{lab}} = 55^\circ$, impurity peaks are not fitted by solid line.

uncertainty of $\pm 15\%$ seems to be realistic. The final absolute error should be an incoherent sum of (a), (b), and (c).

III. DWBA ANALYSIS

In order to determine l -transfer and spectroscopic factors, the experimental angular distributions were compared to DWBA calculations. These calculations were performed with the code DWUCK¹³ (version 08, Aug. 1, 1969) using the nonlocality parameters $\beta_p = 0.85$, $\beta_d = 0.54$, and $\beta_t = 0.25$. For the bound-neutron wave function no nonlocality correction was used. The calculations were carried out with finite range parameters 0.845 and 0.621 for the pickup and stripping reactions, respectively. The optical potential parameters which have been chosen for these DWBA calculations are listed in Table I. Variations of optical parameters with target mass and particle energy—as extracted from the original publications for the potentials—have been included in our DWBA calculations, but these variations are not large and Table I lists only average values for the parameters. The triton optical model parameter set is that of Flynn *et al.*¹⁴ [These parameters are in general agreement with the mass and energy dependent set of

TABLE I. Optical model potential parameters. Potential strengths in MeV, lengths in fm; the parameter of the Coulomb radius was 1.25 fm. The analytical expression of the potential is

$$V = V_C + V_R f(r, R_R, a_R) + V_{so}(S, L) \frac{\hbar}{(m\pi c)^2} \frac{1}{r} \frac{d}{dr} f(r, R_{so}, a_{so}) + iW_I f(r, R_I, a_I) + iW_D A a_I \frac{d}{dr} f(r, R_I, a_I)$$

where:

$$f(r, R_N, a_N) = \{1 + \exp[(r - R_N)/a_N]\}^{-1},$$

$$R_N = r_N A^{1/3}, N = R, I, \text{so}.$$

Particle	V_R	r_R	a_R	W_I	r_I	a_I	W_D	W_{so}	r_{so}	a_{so}	Ref.
Proton	-57.10	1.170	0.750	-1.05	1.320	0.620	9.50	-6.20	1.010	0.750	16
Deuteron 12.5 MeV	-103.32	1.100	0.830		1.309	0.906	13.10	-5.63	0.980	1.000	18
Deuteron 17.0 MeV	-106.63	1.100	0.820		1.249	0.818	15.90	-5.63	0.980	1.000	18
Deuteron 17.0 MeV	-102.00	1.200	0.820		1.310	0.730	14.20				19
Triton	-153.00	1.240	0.700	-16.42	1.420	0.890					14
Bound neutron	a	1.250	0.650								

^a Adjusted by the computer program to fit the neutron separation energy.

Becchetti and Greenlees,¹⁵ which has been used with reasonable success in (p, t) studies on even samarium isotopes.^{10]}

The proton optical parameters are those of Becchetti and Greenlees.¹⁶ (In an elastic scattering experiment at 25 MeV on the even isotopes of samarium this parameter set turned out to be quite useful.¹⁷⁾

In the rare earth region, unfortunately, no well established set of deuteron parameters is available. For this reason two sets have been compared. One is the recently published global fit of Childs, Daehnick, and Spisak (CDS).¹⁸ The other set of deuteron parameters is one which has been used in (d, p) studies¹⁹ on the rare earth nuclei Nd and Ce. Changes in the deuteron spin orbit potential do not significantly affect angular distribution shapes, so it seems that the main difference between the two optical model sets lies in the radius parameter of the real volume term. For $l=3$ transitions both

deuteron parameter sets give quite comparable results. However, significant differences do appear for $l=0$ cases as seen in Fig. 2 where $l=0$ predictions from calculations with the two deuteron potentials are shown for two different excitation energies. The calculation with the CDS parameters shows much less structure for angles greater than 40° for 2.05 MeV excitation energy. Another interesting effect shows up for 4.00 MeV excitation energy where the second minimum at $30-32^\circ$ becomes more shallow in both cases. For the parameter set with the bigger radius parameter however this minimum flattens out to a shoulder.

The DWBA cross sections are strongly dependent on the residual excitation energy. Therefore DWBA calculations were carried out for all interesting l transfers in about 0.5 MeV excitation energy steps and the individual cross sections determined by interpolation. The DWBA calculations have been normalized conventionally by^{13,20}:

$$(d, t) \text{ reaction: } \frac{d\sigma}{d\Omega_{\text{exp}}} = 3.33 \left(\frac{2s+1}{2} \frac{1}{2j+1} \right) \sigma_{ij}(\theta)^{\text{DW}} C^2 S_{ij}$$

$$(d, p) \text{ reaction: } \frac{d\sigma}{d\Omega_{\text{exp}}} = 1.53 \left(\frac{2s+1}{2} \frac{1}{2j+1} \right) \left(\frac{J_f+1}{J_i+1} \right) \sigma_{ij}(\theta)^{\text{DW}} C^2 S_{ij},$$

where $\sigma_{ij}^{\text{DW}}(\theta)$ is the cross section calculated by code DWUCK, S_{ij} is the spectroscopic factor for a specific l_j , s and j represent the spin and the total angular momentum of the transferred neutron, respectively. J_f is the total spin of the final state, whereas J_i is the total spin of the target nucleus ground state. In the present study $J_i = \frac{7}{2}$ both for ^{147}Sm and for ^{149}Sm .

IV. RESULTS

In a number of pickup reactions on $N=82$ target nuclei²¹⁻²⁷ it has been shown that the shell closure at $N=82$ is a good approximation in the sense that no measurable components of neutron states from the $82 < N \leq 126$ major shell were observed. In these studies leading to ^{137}Ba , ^{139}Ce , ^{141}Nd , and ^{143}Sm the sequence of neutron single hole energies

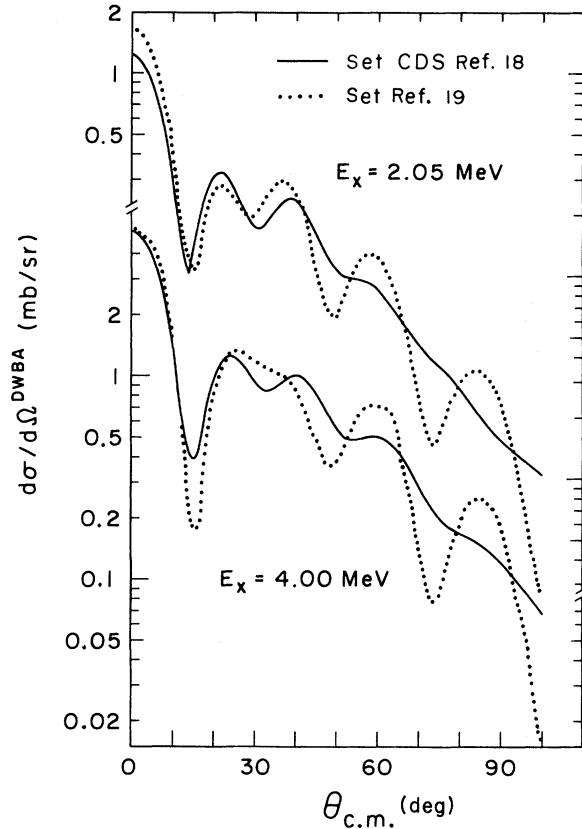


FIG. 2. DWBA calculations for $3s_{1/2}$ neutron pickup. Calculations which use two different deuteron optical model sets at two excitation energies are compared.

has been determined to be $d_{3/2}$ (ground state), $s_{1/2}$, $h_{11/2}$, $d_{5/2}$, and $g_{7/2}$; where the $(2d_{3/2})$ is observed to be a pure hole state, the $(1h_{11/2})$ and the $(3s_{1/2})$ neutron holes fractionated into no more than two components, and the $(2d_{5/2})$ and the $(1g_{7/2})$ are fragmented considerably.

The final nuclei investigated in the present study have two (^{146}Sm) and four (^{148}Sm) neutrons above the closed $N=82$ shell, the targets three (^{147}Sm) and five (^{149}Sm) neutrons. Therefore by shell model considerations the pickup reaction should show spectroscopic strength both for core hole configurations and for removal of neutrons from the $82 < N \leq 126$ major shell, while in the stripping reaction, only this latter shell ought to be observed.

A. Reaction $^{147}\text{Sm}(d,t)^{146}\text{Sm}$

A triton energy spectrum of the reaction $^{147}\text{Sm}(d,t)^{146}\text{Sm}$ at 55° lab angle is shown in Fig. 1. The experimental results are summarized in Table II along with other relevant data for comparison.^{10, 28, 29} Angular distributions for this reaction are shown in Figs. 3 through 9. Below 2 MeV excitation energy the four strongest peaks corre-

pond to the members of the ground state band up to the 6^+ state at 1.811 MeV excitation energy. The state at 1.648 MeV excitation energy is the 2^+ state of the quasi γ band. The $l=3$ strength is almost exhausted in the first six levels below the energy gap, with the exception of the 2.533 MeV state (No. 27), whose experimental angular distribution could only be fitted by a linear combination of $l=1$ and $l=3$ DWBA predictions, as is seen in Fig. 3. This figure includes two further angular distributions which could only be described by mixtures of $l: l=1+l=3$ for the 0.747 MeV state (No. 1) and $l=3+l=5$ for the previously unreported 1.792 MeV state (No. 5).

Whereas both the ground state transition and the transition to the well known 1.811 MeV 6^+ state (No. 6) are described reasonably well by $l=3$ DWBA predictions, the transitions to the states 1.381 MeV (No. 3) and 1.648 MeV (No. 4) require a small amount of additional $l=1$ strength (see Fig. 4). It is known that the 3^- state of the octupole band at 1.381 MeV excitation energy³⁰ is only 1 keV apart from the 4^+ member of the ground state band, see Table II. However, since the spin and parity of the target ground state are known to be $\frac{7}{2}^-$ an even l transfer is expected to populate this negative parity state. Obviously the yield of this state is small

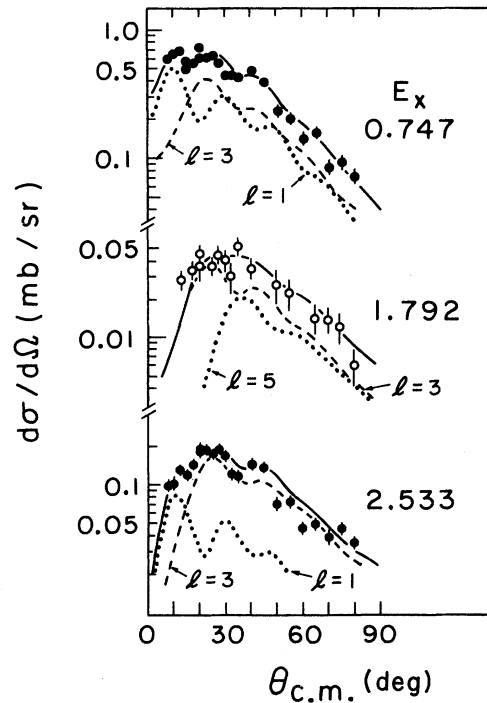


FIG. 3. $^{147}\text{Sm}(d,t)^{146}\text{Sm}$ angular distributions which could only be fitted by mixed l -transfer calculations. The curves represent DWBA predictions. Only statistical errors are included.

TABLE II (Continued)

No.	Ref. 2		Ref. 5		Ref. 28		Refs. 10 and 29		Present (d, t) work				π final state	
	E_x (MeV)	J^π	E_x (MeV)	J^π	E_x (MeV)	J^π	max. rel. int.	E_x (MeV)	J^π	dom. 1	$\frac{d\sigma}{d\Omega}$ max.	C^2S_{ij}		J limits
34	2.679		2.680	3^-	2.681				2.682		c			
35									2.711		c			
36	2.726													
37	2.739				2.738		0.03		2.787	(2)	0.07	0.04	(1-6)	(-)
38					2.786									
39	2.799													
40					2.808									
41									2.829	0	0.04	0.01	3,4	-
42	2.851				2.851				2.856	b	0.04			
43	2.899		2.899						2.899	1	0.29	0.05	2-5	+
44			2.904						2.903		c			
45	2.932				2.933				2.933	b	0.06			
46	2.972				2.979				2.971	0	0.20	0.06	3,4	-
47					2.998				2.995	b	0.03			
48	3.015								3.017	b	0.08			
49	3.028				3.021			3.040 (0^+)	0.08					
50	3.056				3.056									
51	3.072				3.071				3.069 ^d	1	0.22	0.04	2-5	+
52									3.101		c			
53	3.138								3.138	2	0.36	0.25	1-6	-
54			3.168											
55	3.186				3.187				3.188	b	0.12			
56									3.224 ^a	(5)	0.15	0.89	(1-9)	(+)
57	3.239				3.240				3.244	b	0.12			
58	3.260				3.264				3.269		c			
59	3.335								3.335	b	0.08			
60									3.367	0	0.78	0.26	3,4	-
61									3.395	0	0.60	0.21	3,4	-
62														
63	3.419								3.425	b	0.60			
64									3.438	0	0.52	0.18	3,4	-
65									3.473	b	0.08			
66									3.496 ^d	2	1.22	1.03	1-6	-
67									3.526 ^d	0	0.14	0.05	3,4	-
68									3.551 ^d	b	0.06			
69									3.588	0	0.62	0.23	3,4	-

TABLE II (Continued)

No.	Ref. 2		Ref. 5		Ref. 28		Refs. 10 and 29		Present (d, t) work		π final state	
	E_x (MeV)	J^π	E_x (MeV)	J^π	E_x (MeV)	J^π	E_x (MeV)	J^π	dom. 1	$\frac{d\sigma}{d\Omega}$ max.		C^2S_{ij}
70									0	0.68	0.26	3, 4
71									b	0.12		
72									b	0.17		
73	3.728								0	0.12	0.05	3, 4
74									0	0.60	0.25	3, 4
75	3.785											
76									0	0.68	0.29	3, 4
77									0	0.08	0.04	3, 4
78									b	0.04		
79									b	0.02		
80												
81									0	0.13	0.05	3, 4
82									b	0.06		
83									0	0.29	0.14	3, 4
84									b	0.06		
85									b	0.20		
86									0	0.12	0.06	3, 4
87									b	0.10		
88									b	0.04		
89									(5)	0.09	0.93	(1-9)
90									b	0.05		
91									b	0.08		
92									b	0.06		
93									b	0.10		
94									b	0.07		
95									b	0.09		
96									b	0.15		
97									b	0.10		
98									b	0.08		
										c		

^a See text for these levels.

^b Levels could not be assigned to a unique l transfer or a plausible l mixture.

^c Levels weakly populated, $d\sigma/d\Omega_{\text{max}} \leq 0.02$ mb/sr.

^d These levels assigned here as one state seem to be unresolved doublets, less than 10 keV apart from each other.

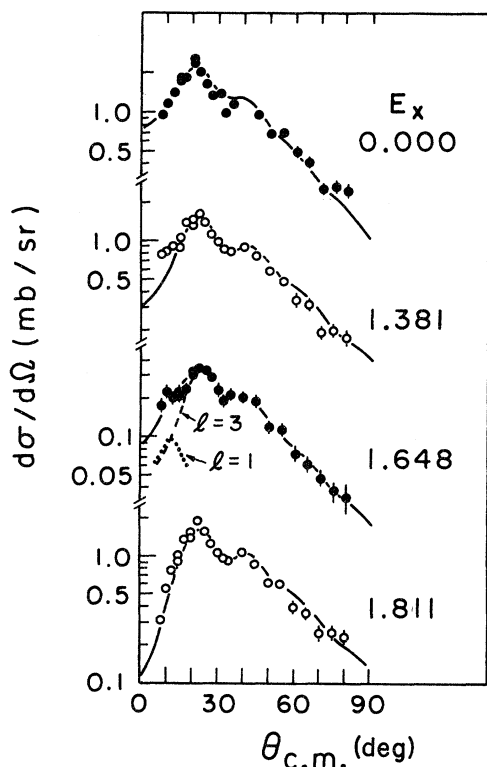


FIG. 4. $^{147}\text{Sm}(d,t)^{146}\text{Sm}$ angular distributions with dominant $l=3$ strength. The curves represent DWBA predictions. Only statistical errors are included.

relative to the observed 4^+ state, because no addition of an even l DWBA angular distribution could improve the fit shown in Fig. 4.

In order to give an idea what the DWBA predictions of the angular distributions depending on different l values look like the most likely examples for the investigated mass region are collected in Fig. 5.

As can be seen from Table II and from the triton energy spectrum in Fig. 1 there is a region between 1.9 and 3.3 MeV excitation energy in the final nucleus ^{146}Sm , which shows 37 rather weakly populated states. Fifteen of these states are observed with a maximum cross section ≤ 0.02 mb/sr. Since our observation limit due to counting statistics, background, and automatic plate scanning was on the order of 0.01 mb/sr, the experimental angular distributions of these states are fairly unreliable and are therefore neither shown nor further discussed in the present paper.

Four states in this weak yield region (between 1.9 and 3.3 MeV excitation energy) are populated by pure $l=1$ transfer. The experimental angular distributions including DWBA predictions for $3p_{3/2}$ pickup are shown in Fig. 6 and seem to be quite reliable. Apart from a contribution of $l=1$ transfer

in populating the 2.533 MeV state (No. 27) the only further $l=1$ spectroscopic strength is observed in the transition to the 2.156 MeV state (No. 15). The angular distribution of this state is included in Fig. 7. This figure represents the $l=0$ transitions, the first six of them lying at less than 3.3 MeV excitation energy. As can be seen, the 2.156 MeV angular distribution deviates from the others in the region of the first minimum at 15° . Populated by $l=0$ the 2.156 MeV state is expected to have spin and parity 3^- or 4^- . However, at 2.157 MeV a 2^+ state (quasi β band) is reported,^{5,30} see Table II, and in fact by adding an $l=1$ contribution the experimental angular distribution can be fitted quite well. This result has been included in Table II.

Eight experimental angular distributions in the excitation energy range of 2 and 3.3 MeV could not be fitted and are displayed in the first part of Fig. 8.

Three $l=2$ transitions are observed near an excitation energy of 3.3 MeV. Their angular distributions are shown in Fig. 9 and compared to DWBA calculations for $2d_{3/2}$ neutron pickup.

Of the remaining 37 states observed up to an excitation energy of 4.5 MeV 12 are not displayed. Either the yield was too low to get reasonable angular distributions or the uncertainty due to the background and level density in conjunction with the energy resolution was too high. In fact only $l=0$ transitions could be assigned uniquely above 3.5 MeV excitation energy. These $3s_{1/2}$ pickup angular distributions are collected in Fig. 7. The DWBA fits are not outstanding but seem to be reasonable. Obviously the worst case is seen for the 3.367 MeV state (No. 60).

Finally, in the second part of Fig. 8 angular distributions are shown which could not be associated with a unique l transfer or a simple linear combination of l 's. Their excitation energy lies above 3.4 MeV. The states at 3.224 MeV (No. 56) and 4.174 MeV (No. 88) excitation energy seem to include some $l=5$ strength and the $1h_{11/2}$ pickup DWBA predictions are included in Fig. 8 for these states. Comparing the experimental angular distribution to DWBA calculations no further evidence for higher l transfer ($l>3$) could be clearly observed.

B. Reaction $^{149}\text{Sm}(d,t)^{148}\text{Sm}$

A triton energy spectrum of the reaction $^{149}\text{Sm}(d,t)$ at 55° lab angle is shown in Fig. 1. The experimental results are summarized in Table III along with other published^{10,29,31} and our stripping data to ^{148}Sm . The energy spectra have been analyzed up to 4 MeV excitation energy.

Comparing the triton energy spectra in Fig. 1 it is obvious that in the case of ^{148}Sm the level

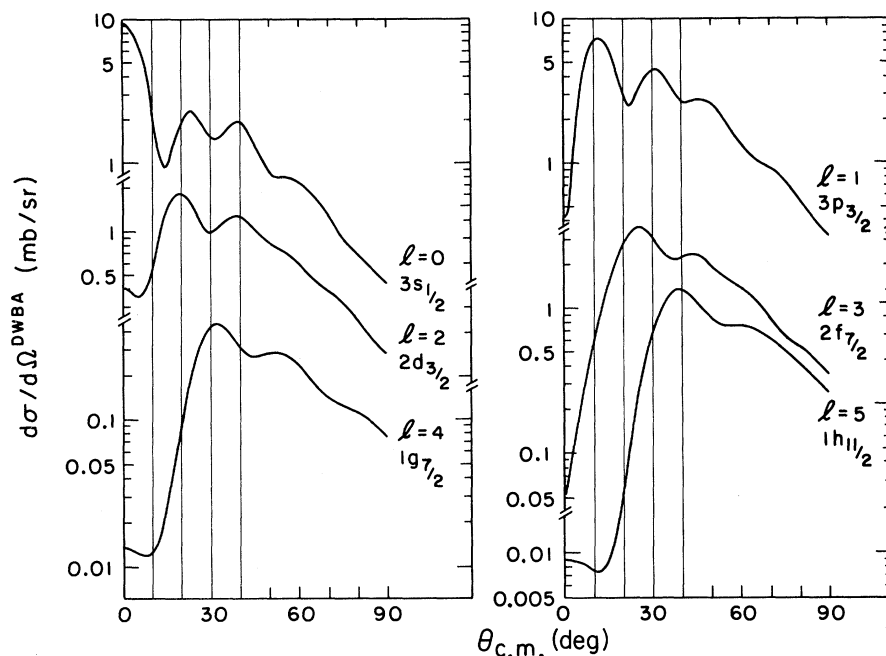


FIG. 5. The most likely l -transfer DWBA calculations for the reaction $^{147}\text{Sm}(d, t)$ and 3 MeV excitation energy.

density is much higher and the yield in the former rather weakly populated region ($1.9 \text{ MeV} \leq E_x \leq 3.3 \text{ MeV}$) is now stronger.

Below 2 MeV excitation $l=3$ is the dominant transfer. The angular distributions of these levels along with four $l=3$ transitions higher in excitation energy are shown in Fig. 10 and are fitted quite well in all 11 cases by DWBA calculations for $2f_{7/2}$ pickup. Contrary to the case of $^{147}\text{Sm}(d, t)^{146}\text{Sm}$, in the reaction leading to ^{148}Sm the main $l=3$ strength is not limited to the excitation energy range below the energy gap.

Additional $l=3$ transfer mixed with $l=1$ strength has been seen in three levels. The corresponding angular distributions are shown in Fig. 11. As in the analysis of any mixed l transitions the ratios of $l=1$ to $l=3$ strengths in these cases are somewhat uncertain; however, the mixtures reported here do fit the experimental angular distributions fairly well.

Pure $l=1$ transitions have been observed in nine cases and these are shown with DWBA calculations in Fig. 12. It is obvious that the second maximum of the $l=1$ angular distributions (at $25\text{--}28^\circ$) is more pronounced in the experimental data than in the theoretical curves. This was not the case for the $l=1$ angular distributions seen in the $^{147}\text{Sm}(d, t)$ reaction (Fig. 6).

Figure 13 presents the angular distributions of states which are predominantly populated by $l=0$ transfer. The 1.162 MeV state (No. 2) is known

to have spin and parity 3^- , so an $l=0$ transition would be likely. However, the counting statistics of this rather weakly excited state are poor and an $l=2$ contribution cannot be excluded. The next 12 angular distributions in Fig. 13 (excitation energy 2.035 to 4.026 MeV) seem to be well reproduced by $l=0$ pickup calculations. The remaining 15 distributions (excitation energy 2.117 to 3.990 MeV) are probably dominated by $l=0$ transitions; however, some deviations from the ideal $l=0$ angular distribution shape are visible. These deviations may be due (a) to $l=2$ mixtures, which are likely because no pure $l=2$ transfer has been observed in the $^{149}\text{Sm}(d, t)$ case or (b) to unresolved levels (see e.g. Table III level Nos. 22 and 23).

Finally, in Figs. 14 and 15 those experimental angular distributions are presented which could not be associated with a unique l transfer or a plausible mixture of l values. All the data of Fig. 14 show a similar behavior in the sense that the angular distributions are characterized by a minimum at $15\text{--}20^\circ$, increase to a maximum at $25\text{--}30^\circ$ and fall exponentially towards higher angles. Comparing this general structure to DWBA calculations (see Fig. 5) the minimum at $15\text{--}20^\circ$ could only be explained by $l=0$ transfer, whereas the position of the maximum indicates more an $l=3$ type of transfer.

A different type of undetermined angular distribution is given in Fig. 15. These data typically show a more or less constant cross section from

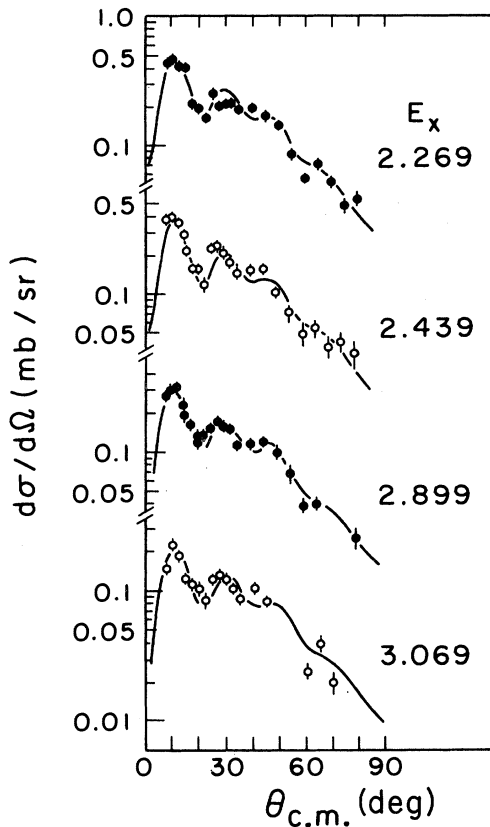


FIG. 6. $^{147}\text{Sm}(d,t)^{146}\text{Sm}$ angular distributions with dominant $l=1$ strength. The curves represent DWBA predictions. Only statistical errors are included.

7 to about 40° and decrease from 40 to 65° by a factor of 4–5. The latter property is in agreement with the DWBA predictions for all l transfers (shown in Fig. 5) so combinations of $l=1$, $l=3$, and $l=5$, for instance, can produce such types of angular distributions. It is quite an open question how reliable higher l -value DWBA calculations are for the energy range of the present experiment. However, (d,t) investigations done in this laboratory^{32,33} and elsewhere³⁴ on rare earth nuclei leading to odd neutron number final nuclei using 17 MeV or even lower energy deuterons show $l>3$ experimental angular distributions which agree well with DWBA predictions. Thus the lack of evidence for higher l transfer in our experiment is not understood.

C. Reaction $^{147}\text{Sm}(d,p)^{148}\text{Sm}$

The third reaction we present here is the one-neutron stripping reaction $^{147}\text{Sm}(d,p)^{148}\text{Sm}$. The results are listed in Table III and angular distributions are shown in Figs. 16 and through 21. A proton energy spectrum is shown in Fig. 1 at 55° lab angle. The yield as a function of excitation

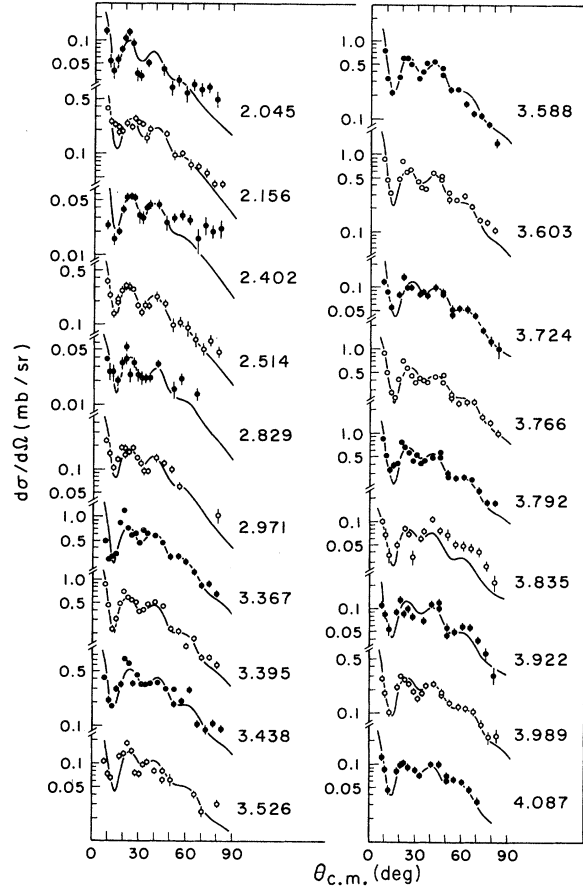


FIG. 7. $^{147}\text{Sm}(d,t)^{146}\text{Sm}$ angular distributions with dominant $l=0$ strength. The curves represent DWBA predictions. Only statistical errors are included.

energy is nearly opposite to that seen in the (d,t) reaction. Among all members of the ground state band only the 6^+ state (1.906 MeV, No. 14) is strongly excited. Unfortunately some impurities (indicated by not being fitted in Fig. 1) mask some states, for instance the peak No. 4 which corresponds to a level of 1.427 MeV excitation energy. This state is observed with a fairly constant cross section of 0.02 mb/sr between 20 and 80° .

The stripping reaction populates states strongly in the region between 1.9 and 3.3 MeV. This leads to the conclusion that in this excitation energy range above the energy gap the quasiparticle character is dominant. We observed 42 levels in the (d,p) reaction up to an excitation energy of 3.5 MeV. Eight angular distributions are not shown, because (a) the yield was too small or (b) the levels appear to be unresolved and seem to be composed of more than one nuclear state.

According to the shell model considerations outlined in the beginning of this section this (d,p) reaction should populate single particle configura-

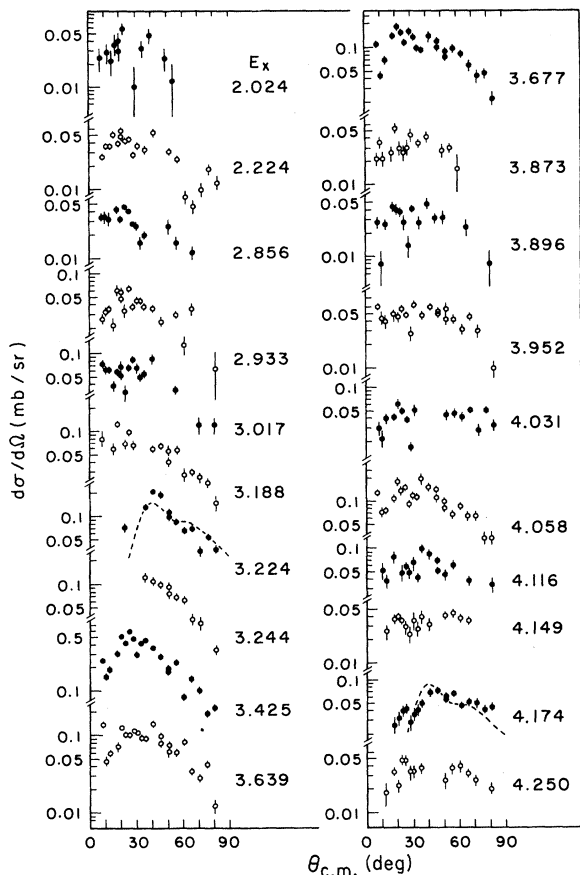


FIG. 8. $^{147}\text{Sm}(d, t)^{146}\text{Sm}$ experimental angular distributions which could not be fitted by DWBA calculations. Only statistical errors are included. The dotted lines show $l=5$ DWBA predictions.

tions in the $82 > N \geq 126$ major shell. This means f , h , p , and i strength should be observed. However, as in the (d, t) cases discussed above, no significant h or i strength is observed in this (d, p) investigation. This result is puzzling since a survey of publications^{19, 35, 36} investigating the one-neutron stripping process to final $N=83$ and $N=85$ nuclei indicated that some $l=5$ and $l=6$ strength has usually been observed below 2 MeV excitation energy. On the other hand, the higher l transitions are intrinsically weaker than low l transitions and, in the case of an odd mass target, the high l strength might be highly fragmented so it may be reasonable that such strength would not be observed in the present work. Further, Ascuitto, Vaagen, King, and McVay^{7, 37} have reported evidence for higher order processes in single nucleon transfer reactions. By using coupled-channel Born approximation calculations they successfully fit experimental (p, d) angular distributions in the rare earth region and their fits for high l transitions bear strong resemblance to the four structureless

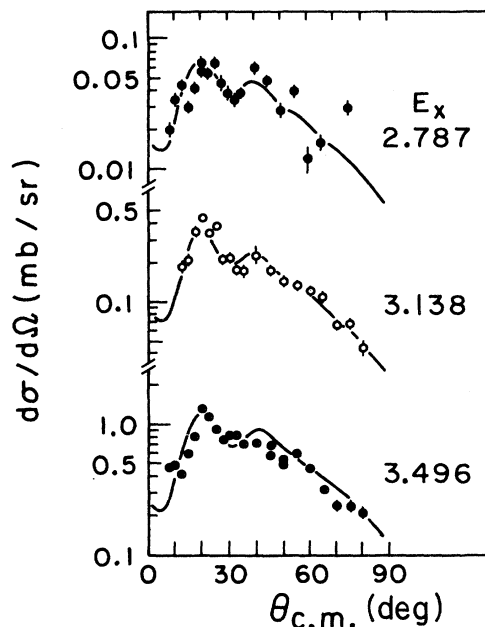


FIG. 9. $^{147}\text{Sm}(d, t)^{146}\text{Sm}$ angular distributions with dominant $l=2$ strength. The curves represent DWBA predictions. Only statistical errors are included.

angular distributions shown in Fig. 16.

In this (d, p) study 29 levels have been observed to show at least dominant $l=3$, $l=1$, and $l=1+3$ contributions. These are shown in Figs. 17–20. Figure 17 shows angular distributions which are dominated by $l=3$ transfer with possible small contributions of $l=1$, Fig. 18 a comparable strength of $l=1$ and $l=3$, Fig. 19 dominant $l=1$ plus small amounts of $l=3$, and finally Fig. 20 apparently pure $l=1$ transfer. All fits seem to be quite reliable even though a considerable uncertainty is introduced by the mixing of $l=1$ and $l=3$.

Figure 21 shows the 1.163 MeV (No. 2) angular distribution. This state is known to have spin and parity 3^- and therefore it is expected to be excited by an even l transfer (target spin $=\frac{7}{2}^-$). It seems that the $2d_{3/2}$ orbit is responsible for its reasonably weak population in this experiment.

V. SPECTROSCOPIC INFORMATION

The sum of the spectroscopic factors for the reactions $^{147, 149}\text{Sm}(d, t)$ are given as a function of excitation energy in Fig. 22. For the $l=3$ transitions the spectroscopic strength is essentially the same for both cases up to an excitation energy of about 1.9 MeV (probably just the gap energy). Above the energy gap there is only an additional 5% $l=3$ strength in the reaction $^{147}\text{Sm}(d, t)$ and the sum of the $l=3$ spectroscopic factor is 2.3. In the reaction $^{149}\text{Sm}(d, t)$, however, above the gap energy the sum of the spectroscopic factors is 1.9, which

TABLE III (Continued)

E_x (MeV)	dom. 1	(d, p) results		Present work				C^2S_{1j}	J limits	π final state			
		$\frac{d\sigma}{d\Omega}$ (mb/sr)	max.	$(2J_f+1)C^2S_{1j}$	E_x (MeV)	dom. 1	$\frac{d\sigma}{d\Omega}$ (mb/sr)				max.		
0.000	3	0.07		2.11		0.000	3	2.25	0.61	0-7	+		
0.551	1, 3	0.18	0.04	1.14	1.12	0.550	3	0.96	0.33	2-5	+		
1.163	2	0.02		0.39		1.162	0	0.06	0.01	3, 4	-		
1.181	1, 3	0.06	0.04	0.34	1.06	1.181	3	1.00	0.41	2-5	+		
1.427 ^a		b				1.456	1	0.54	0.07	2-5	+		
1.666	3	0.06		1.46		1.666	3	0.38	0.19	0-7	+		
1.736	1, 3	0.09	0.14	0.49	3.15	1.736	3	1.18	0.60	2-5	+		
						1.898	3	0.56	0.30	0-7	+		
1.906 ^c	1, 3	0.10	0.42	0.56	9.10	1.910	3	1.35	0.74	0-7	+		
1.976	1, 3	0.10	0.03	0.56	0.64	1.976	1	0.45	0.06	2-5	+		
						2.035	0	0.04	0.01	3, 4	-		
2.100	1, 3	0.02	0.15	0.10	3.14	2.099	3	0.75	0.43	2-5	+		
2.116	d	0.06				2.117	(0)	0.13	0.03	(3, 4)	(-)		
2.151	1, 3	0.10	0.04	0.54	0.87	2.151	1, 3	0.42	0.30	0.05	0.18	2-5	+
2.199	3	0.09		1.85		2.198	3	0.46	0.28	0-7	+		
2.218	1, 3	0.10	0.04	0.51	0.78	2.218	1	0.43	0.06	2-5	+		
2.233	1, 3	0.05	0.02	0.26	0.41	2.232	d	0.20		2-5	+		
						2.277	3	0.06	0.03	0-7	+		
2.318	d	0.08				2.318	1	0.10	0.01	2-5	+		
2.333	1	0.13		0.69		2.331	1, 3	0.06	0.04	0.01	0.03	2-5	+
						2.344	0	0.21	0.05	3, 4	-		
2.379	3	0.17		3.39		2.380	3	0.32	0.21	0-7	+		
2.395	1	0.26		1.34		2.396	1	0.43	0.06	2-5	+		
						2.473	d	0.20					
2.496	1	0.27		1.41		2.496	1	0.42	0.06	2-5	+		
										2-5	+		
2.532	1	0.54		2.81		2.531 ^c	1	0.96	0.14	2-5	+		
						2.574	d	0.08					

TABLE III (Continued)

E_x (MeV)	dom. 1	(d, p) results		Present work				J limits	π final state
		$\frac{d\sigma}{d\Omega}$ (mb/sr) max.	$(2J_f+1)C^2S_{ij}$	E_x (MeV)	dom. 1	(d, t) results $\frac{d\sigma}{d\Omega}$ (mb/sr) max.	C^2S_{ij}		
2.649	1	0.40	2.06	2.646	1	0.26	0.04	2-5	+
				2.683	d	0.06			
2.705	1, 3	0.08 0.04	0.41 0.67	2.705	1, 3	0.10 0.06	0.02 0.04	2-5	+
2.729	1, 3	0.20 0.09	1.03 1.70	2.720	(0)	0.19	0.05	(3, 4)	(-)
2.760 ^c	1, 3	0.10 0.05	0.50 0.85	2.731	d	0.40		2-5	+
				2.759	d	0.10		2-5	+
2.809 ^c	d	0.08							
				2.821 ^c	1	0.25	0.04	2-5	+
2.824 ^c	d	0.07							
				2.843	(0)	0.03	0.01	(3, 4)	(-)
2.868	1	0.11	0.55	2.866	d	0.09		2-5	+
				2.906	0	0.13	0.04	3, 4	-
				2.927	d	0.12			
2.930 ^c	1, 3	0.13 0.07	0.66 1.28	2.936	d	0.05		2-5	+
				2.952	b				
2.989	d } d }	0.15		2.989 ^c	d	0.10			
3.001				2.993 ^c	d	0.08			
				3.006 ^c	d	0.18			
3.022	d	0.08		3.017	0	0.27	0.08	3, 4	-
3.046	1, 3	0.18 0.05	0.90 0.93	3.044	d	0.20		2-5	+
				3.055 ^c	d	0.16			
				3.073 ^c	d	0.08			
				3.098	(0)	0.12	0.04	(3, 4)	(-)
3.112	1, 3	0.10 0.07	0.50 1.16	3.113	d	0.20		2-5	+
				3.138	b				
3.154	1, 3	0.06 0.09	0.31 1.50	3.153	d	0.06		2-5	+
3.178	1, 3	0.13 0.05	0.63 0.84	3.175	d	0.08		2-5	+
				3.198	0	0.11	0.03	3, 4	-
				3.226	d	0.09			
3.243	1, 3	0.12 0.04	0.58 0.73	3.247	d	0.08		2-5	+
				3.274	d	0.06			
				3.313	b				
3.307		b		3.344	d	0.10			
3.349	1	0.28	1.35	3.385	0	0.26	0.09	3, 4	-
				3.397	d	0.20			
3.409	d	0.10		3.405	b				
				3.417	d	0.28			
				3.428	d	0.40			
				3.449	d	0.70			
				3.463	d	0.90			
3.479	d	0.08							
				3.488	(0)	0.19	0.07	(3, 4)	(-)
				3.504	d	0.30			
				3.530	(0)	0.30	0.11	(3, 4)	(-)
				3.546	(0)	0.47	0.17	(3, 4)	(-)
				3.572	d	0.30			
				3.600	(0)	0.19	0.07	(3, 4)	(-)
				3.628	(0)	0.37	0.14	(3, 4)	(-)

TABLE III (Continued)

No.	Ref. 2		Ref. 3		Refs. 10 and 29		Ref. 31		
	E_x (MeV)	J^π	E_x (MeV)	J^π	E_x (MeV)	J^π	rel. max. int.	E_x (MeV)	rel. max. int.
103								3.658	} 4.10
104									
105								3.668	
106									} 4.20
107								3.712	
108								3.734	
109									} 5.55
110								3.761	
111								3.780	
112								3.794	
113									} 4.00
114								3.847	
115									} 2.37
116								3.890	
117									} 0.93
118								3.924	
119								3.953	3.50
120									} 2.20
121								3.990	
122									} 6.00
123								4.028	
124								4.043	
125								4.085	} 6.10
126								4.107	
127									} 24 levels up to $E_x = 4.876$ MeV
128									
to									
151									

^aSee text for these levels.

^bLevels weakly populated, $d\sigma/d\Omega_{\max} \leq 0.02$ mb/sr.

adds to a total sum of approximately 4.4 for this reaction.

The $l=1$ transition strength shows the following behavior: Up to the energy gap in both reactions about 0.06 neutrons are observed; in $^{147}\text{Sm}(d, t)$ the spectroscopic sum adds up to a total of about 0.3, whereas in $^{149}\text{Sm}(d, t)$ a total of 0.6 p neutrons are observed. Out of the three neutrons above the $N=82$ closed shell in ^{147}Sm 2.6 have been observed and only 10% of this strength appears above the energy gap. In $^{149}\text{Sm}(d, t)$ the sum of the spectroscopic strength for $l=3$ and $l=1$ adds up to five neutrons and 40% of this strength appears above the gap energy. Thus our data indicate that ^{149}Sm may be described as ^{147}Sm plus a one quasi neutron pair. This observation is consistent with the (p, t) study³⁸ on ^{149}Sm where only the ^{147}Sm ground state is strongly excited despite a strong fragmentation of (p, t) strength in other neighboring odd-mass

isotopes.

The lower part in Fig. 22 shows $l=0$ transition strength which is in both cases essentially equivalent and shows the total expected $3s_{1/2}$ subshell. As can be seen from the figure the $l=0$ strength starts at high excitation energy which again indicates the good approximation of shell closure at $N=82$.

Additionally, $l=2$ spectroscopic strength has been observed only in the reaction $^{147}\text{Sm}(d, t)$. The sum of the spectroscopic factors for $l=2$ strength is 1.3 for the levels at 2.787 MeV (No. 38), 3.138 MeV (No. 53), and 3.496 MeV (No. 66) excitation energy. It remains, however, a question why the $2d$ strength seems to be that much suppressed, since the $2d_{3/2}$ orbit is expected to close the $N=82$ shell (see above). As discussed above it is quite possible that at least some of this strength is hidden in small admixtures to the $l=0$ angular distri-

TABLE III (Continued)

E_x (MeV)	dom. 1	Present work		E_x (MeV)	dom. 1	$\frac{d\sigma}{d\Omega}$ (mb/sr) max.	C^2S_{lj}	J limits	π final state
		(d, p) results $\frac{d\sigma}{d\Omega}$ (mb/sr) max.	$(2J_f+1)C^2S_{lj}$						
				3.652	(0)	0.25	0.09	(3, 4)	(-)
				3.674	d	0.14			
				3.696	(0)	0.27	0.10	(3, 4)	(-)
				3.714	d	0.10			
				3.734	(0)	0.12	0.05	(3, 4)	(-)
				3.752	d	0.12			
				3.774	(0)	0.28	0.11	(3, 4)	(-)
				3.797	d	0.11			
				3.817	0	0.21	0.09	3, 4	-
				3.843	0	0.21	0.09	3, 4	-
				3.862	0	0.31	0.13	3, 4	-
				3.888	d	0.12			
				3.902	0	0.12	0.05	3, 4	-
				3.924	0	0.39	0.17	3, 4	-
				3.951 ^c	d	0.14			
				3.975	(0)	0.18	0.08	(3, 4)	(-)
				3.990	(0)	0.09	0.04	(3, 4)	(-)
				4.005	d	0.04			
				4.011	b				
				4.026	0	0.15	0.07	3, 4	-
				4.041	d	0.08			

^cThese levels assigned here as one state seem to be unresolved doublets, less than 10 keV apart from each other.

^dLevels could not be assigned to a unique l transfer or a plausible l mixture.

butions. Additionally, this observation may indicate a continuation of the previously reported²¹ decrease in the $d_{3/2}-s_{1/2}$ energy gap among the $N = 81$ nuclei Ba, Ce, and Nd as the $d_{5/2}$ proton shell is filling, and among the $N = 83$ nuclei Nd and Ce.¹⁹ Unfortunately there are no extensive one-nucleon transfer studies to even-even rare earth isotopes available with which to compare this data.

Only in the $^{147}\text{Sm}(d, t)$ reaction could we observe some $l = 5$ transition strength [which adds up to a total spectroscopic factor of 1.8 for the levels at 1.792 MeV (No. 5), 3.224 MeV (No. 56), and 4.174 MeV (No. 88) excitation energy]. The angular distributions and DWBA fits of the levels containing $l = 5$ strength are shown in Figs. 3 and 8. As discussed above, these fits yield highly uncertain spectroscopic factors.

In both the stripping and the pickup reactions to the final nucleus ^{148}Sm no $l = 5$ transitions have

been found. As discussed above: (1) high l angular distributions are of intrinsically low cross section and so their contributions tend to be lost in mixed l transitions and (2) the presence of multistep processes could distort angular distribution shape making it difficult to identify the $l = 5$ contributions. The following conclusions may be made, however: In both (d, t) cases neither the $h_{9/2}$ nor the $i_{13/2}$ subshell (both of which should lie above the target Fermi surface) contributes substantially to the ground state wave function. The main expected $h_{11/2}$ spectroscopic strength is deeply bound and therefore probably inaccessible to our experiment.

Comparing the low lying levels of our (d, t) results (Tables II and III) it is obvious that in the case of $^{149}\text{Sm}(d, t)$ most of the angular distributions could be described by unique l transfers, whereas in $^{147}\text{Sm}(d, t)$ some appeal to l mixing was necessary in order to fit the experimental data.

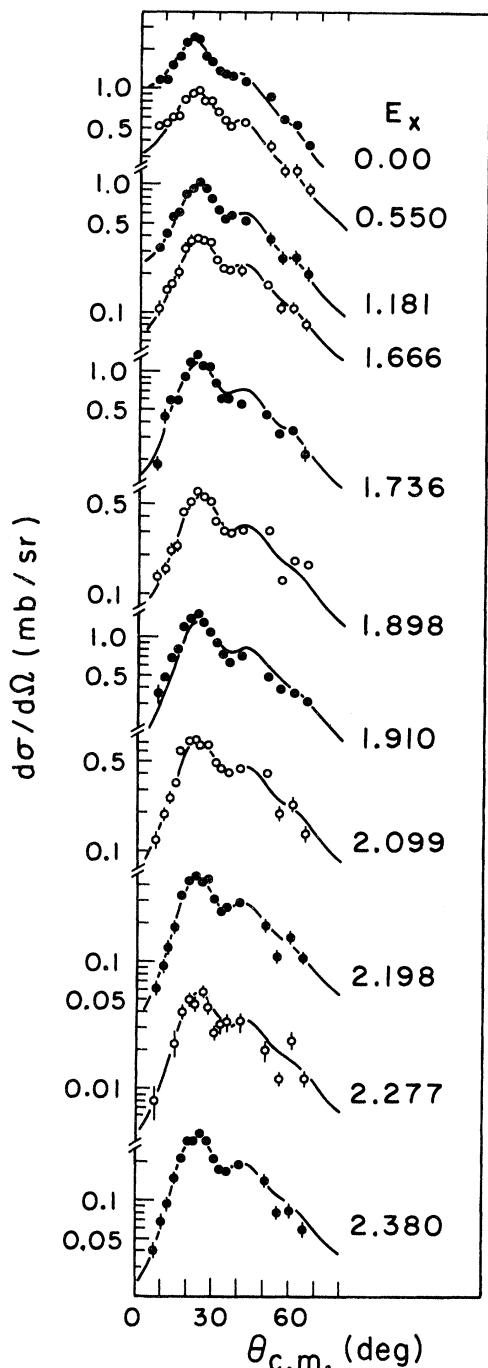


FIG. 10. $^{149}\text{Sm}(d,t)^{148}\text{Sm}$ angular distributions with dominant $l=3$ strength. The curves represent DWBA predictions. Only statistical errors are included.

Hardly any $^{147}\text{Sm}(d,p)$ transitions could be fitted with unique l DWBA angular distribution, as seen from Table III and the figures showing the (d,p) data. With the exception of the 3^- 1.163 MeV state (No. 2) only $l=1$ and $l=3$ transitions have been ob-

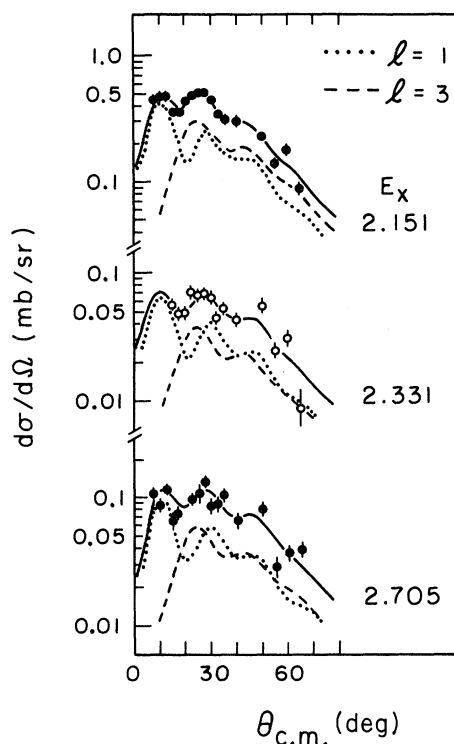


FIG. 11. $^{149}\text{Sm}(d,t)^{148}\text{Sm}$ angular distributions with $l=1+3$ strength. The curves represent DWBA predictions. Only statistical errors are included.

served. The spectroscopic information is summarized in Fig. 23. It seems that all expected $l=3$ strength (five neutron holes in $^{147}\text{Sm} f_{7/2}$ shell) is observed, but only about 70% of the $l=1$ strength up to 3.35 MeV excitation energy. While any one spectroscopic factor may have an error $\approx 30\%$, the comparison of summed spectroscopic strengths from a consistent analysis should be sufficiently reliable to make this distinction between 70 and 100% of expected strength a meaningful one. The main spectroscopic contributions for both l transfers are above 1.9 MeV excitation energy as can be seen from Figs. 1 and 23.

This all leads to the conclusion that the low lying states in ^{148}Sm show more hole than particle state character, whereas in the region between about 1.9 and 3.3 MeV quasiparticle state population is dominant. Unfortunately no (d,p) data to ^{146}Sm could be taken, however it seems probable, from the triton energy spectrum in Fig. 1, that the preference of hole states in the low excitation energy region and of particle character in the region above the energy gap is even more pronounced in the $N=84$ nucleus.

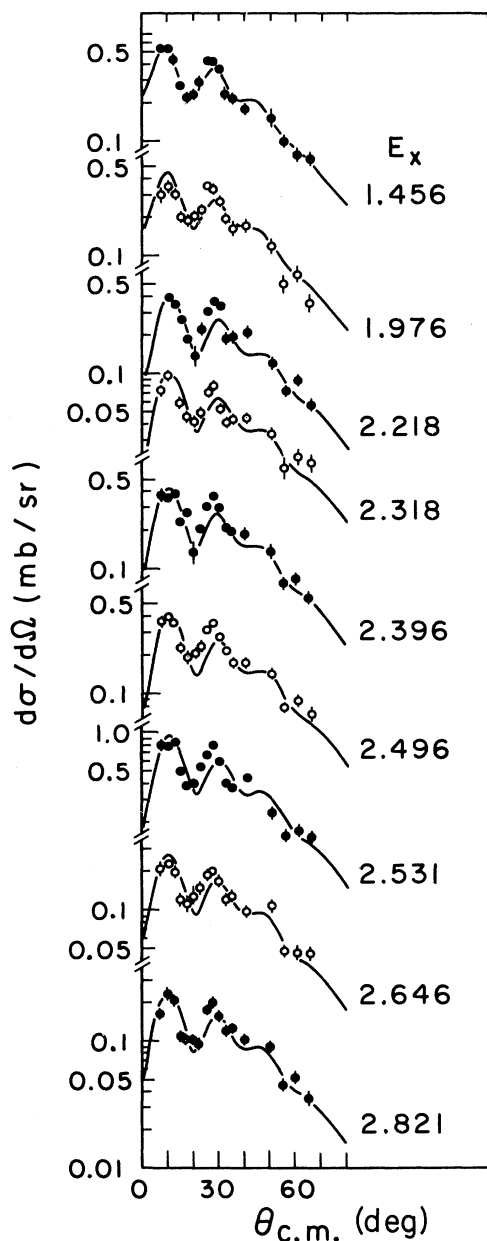


FIG. 12. $^{148}\text{Sm}(d, t)^{146}\text{Sm}$ angular distributions with dominant $l=1$ strength. The curves represent DWBA predictions. Only statistical errors are included.

VI. PHENOMENOLOGICAL COMPARISON TO (p, t) AND (t, p) DATA

A. Ground state band

In this section we try to compare our results to two-nucleon transfer investigations in a phenomenological, collective picture.

For the low lying states (mainly the members

of the ground state band) the following observations of our results are summarized:

(1) In the (d, t) reaction to ^{146}Sm more than 75% of the spectroscopic strength for pickup of neutron configurations from the $82 < N \leq 126$ major shell lies low in the spectrum of ^{146}Sm —below the pairing gap.

(2) In the (d, t) reaction to ^{148}Sm in principle the same observation is valid for three of the five expected neutrons. Remaining strength is observed with a summed spectroscopic factor of $C^2S_{ij} = 2$ above the energy gap.

These two observations suggest a simple terminology which parallels the pairing vibration terminology and which will allow us to discuss qualitative similarities between one- and two-nucleon transfer reaction effects. Neutrons which can be picked up without exciting the residual nucleus to energies above the pairing gap will be called “quasineutrons” and neutron single particle strength which lies at high residual excitation energy will be ascribed to removing a neutron from a “quasineutron pair.”

From this point of view ^{147}Sm might be considered as a ^{144}Sm plus three quasineutron nucleus, ^{149}Sm as a ^{144}Sm plus a quasineutron pair plus three quasineutron nucleus.

(3) Indicated by the dominant hole state character of the low lying states ^{148}Sm might be considered in this terminology as a ^{144}Sm plus a quasineutron pair plus two quasineutron nucleus and ^{146}Sm as a ^{144}Sm plus two quasineutron nucleus.

Investigating the pickup reaction to the ^{146}Sm final nucleus one neutron is removed from the three quasineutrons in ^{147}Sm and two remain and can couple in principle to spin 0, 2, 4, or 6. Accordingly, ^{148}Sm remains in the model configuration as suggested under (3).

In the (d, p) reaction on ^{147}Sm one neutron adds to the proposed ^{147}Sm configuration which would leave ^{148}Sm in a four quasineutron state, but this seems not to be a proper configuration for the low lying levels in ^{148}Sm according to our results.

These observations now agree quite well with phenomena of the two-neutron transfer reactions.^{10, 28, 29} In these reactions it has been observed that (certain restrictions are not discussed here) the first 2^+ states of the $N=84$ and $N=86$ nuclei are strongly populated via the (t, p) reaction, weakly, however, via the (p, t) reaction. By this observation the first 2^+ state has been interpreted to be a quadrupole pairing vibrational state of the addition type (AQP). Using the terminology of Refs. 39–43, this state is specified for the $N=84$ nuclei by $(0, 1_2)$, which transitions is favored by the (t, p) reaction on the $(0, 0)$ ground state target $N=82$. For $N=86$ nuclei it is specified by $(0, 1_0)$

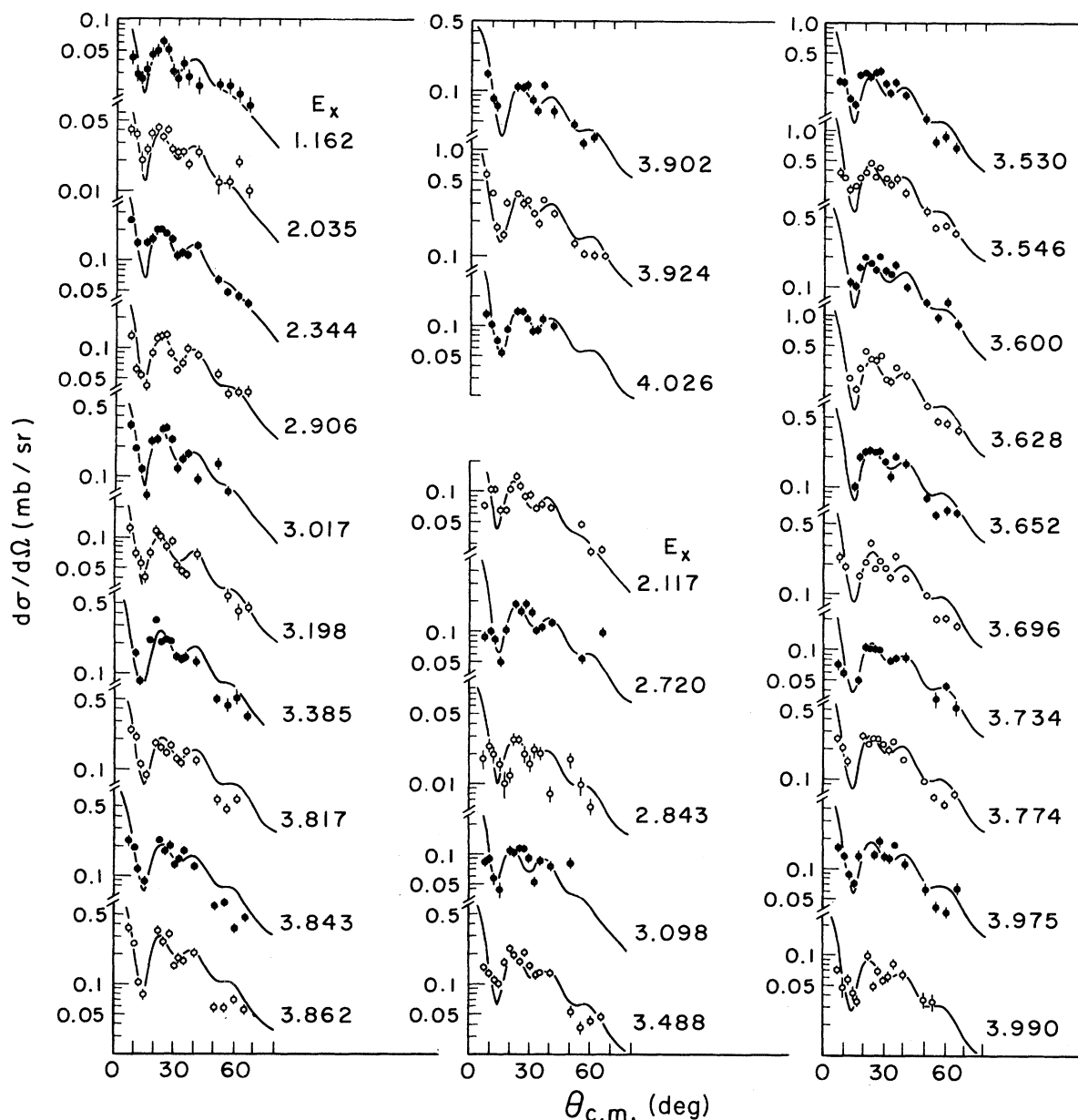


FIG. 13. $^{148}\text{Sm}(d,t)^{148}\text{Sm}$ angular distributions with dominant $l=0$ strength, see text. The curves represent DWBA predictions. Only statistical errors are included.

$(0, 1_2)$ and is again favored by the (t, p) reaction on the $(0, 1_0)$ $N=84$ target.

This description of the first 2^+ state can be extended to other states; in general we describe these states as $(0, 1_n)$ for $N=84$ and as $(0, 1_0)(0, 1_n)$ for $N=86$ nuclei, where n is the spin of the final state and in the investigated mass region $n \leq 6$. [Comparing the results of one- and two-nucleon transfer, the 6^+ state must be consistently excluded from this simple level configuration picture. This state is weakly populated in (p, t) and

in (t, p) reactions, it is, however, strongly excited in both types of one nucleon transfer reactions.]

In relating the one- and two-neutron transfer results we would associate the above defined quasi-neutron pair with the $(0, 1_0)$ notation and the two quasineutrons with $(0, 1_n)$. Structure phenomena observed in the two-nucleon transfer thus seem to be reflected in this one-nucleon transfer study. It would be of certain interest to investigate both the one-nucleon transfer pickup and stripping processes to $N=80$, $N=82$ and $N=84$ final nuclei.

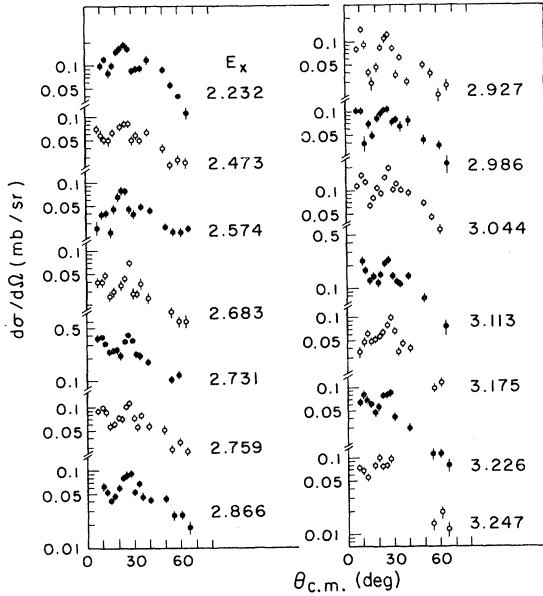


FIG. 14. $^{148}\text{Sm}(d, t)^{148}\text{Sm}$ experimental angular distributions which could not be fitted by DWBA calculations, see text. Only statistical errors are included.

B. Some particular levels

In the last part of this section we compare the yields of some particular levels excited via different reactions. Because ^{146}Sm lies in an unstable region in the chart of nuclides and is unstable itself, it is inaccessible via many reactions. In

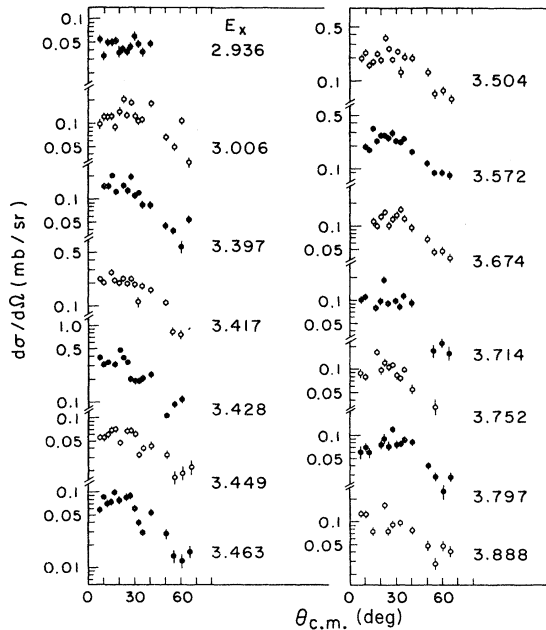


FIG. 15. $^{148}\text{Sm}(d, t)^{148}\text{Sm}$ experimental angular distributions which could not be fitted by DWBA calculations, see text. Only statistical errors are included.

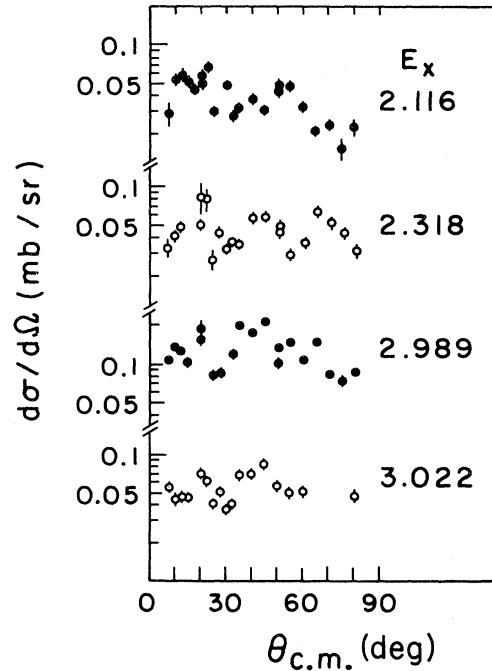


FIG. 16. $^{147}\text{Sm}(d, p)^{148}\text{Sm}$ experimental angular distributions which could not be fitted by DWBA calculations. Only statistical errors are included.

Table II the present (d, t) data are compared with decay studies and two-neutron transfer reactions. Besides the ground state band members, most of the levels observed in the (t, p) reaction are weakly

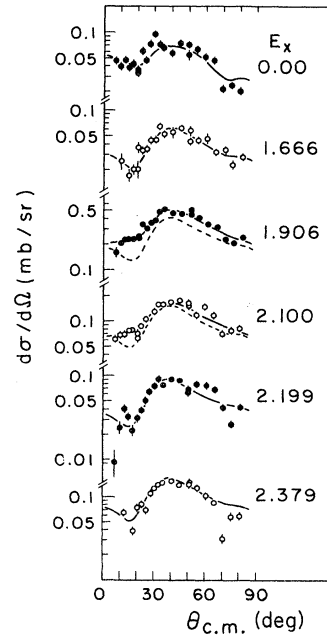


FIG. 17. $^{147}\text{Sm}(d, p)^{148}\text{Sm}$ angular distributions with dominant $l=3$ strength. The curves represent DWBA predictions. Only statistical errors are included.

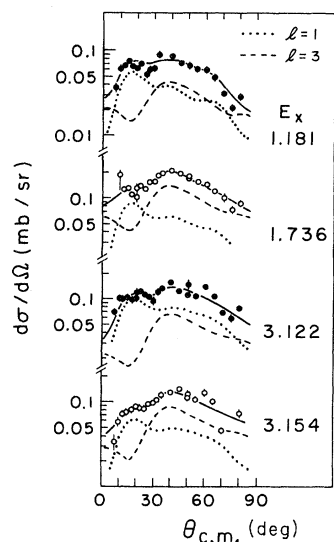


FIG. 18. $^{147}\text{Sm}(d,p)^{148}\text{Sm}$ angular distributions with $l=1+3$ strength. The curves represent DWBA predictions. Only statistical errors are included.

(if at all) populated in (p,t) and (d,t) investigations. Differences in excitation energy or disagreement in parity assignment indicate that two different levels may be involved, as for the states Nos. 21, 22, and 53. From the yield of the 2.442 MeV state (No. 24) in the different reactions a J^π assignment of 4^+ seems most likely. Finally, levels Nos. 33 and 34, populated via the (t,p) reaction are only

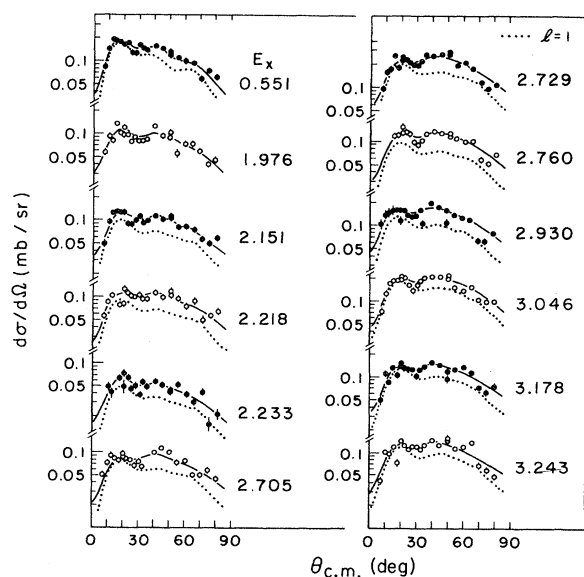


FIG. 19. $^{147}\text{Sm}(d,p)^{148}\text{Sm}$ angular distributions with dominant $l=1$ strength and small $l=3$ contributions. The curves represent DWBA predictions. Only statistical errors are included.

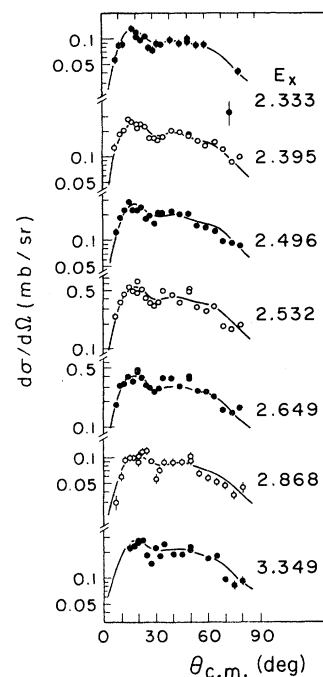


FIG. 20. $^{147}\text{Sm}(d,p)^{148}\text{Sm}$ angular distributions with dominant $l=1$ strength. The curves represent DWBA predictions. Only statistical errors are included.

weakly populated in (d,t) .

For the final nucleus ^{148}Sm (Table III) a similar trend is to be seen. At 1.427 MeV excitation energy in both (p,t) as well as (p,α) studies⁴⁴ a strong level appears. This level has been discussed in terms of shape coexistence arguments and in that picture would be expected to be of less yield in one-nucleon transfer. In fact no significant trace could be observed in the (d,t) study and a very weakly populated state was analyzed in the (d,p) investigation at 1.427 MeV (No. 4). It is uncertain whether this state coincides with the 0^+ state observed in the (p,t) reaction or with the

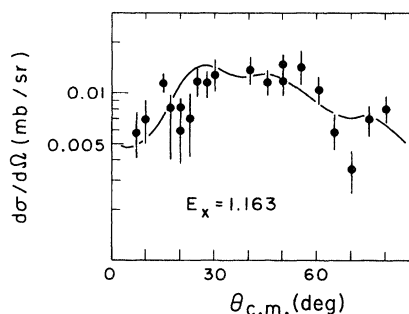


FIG. 21. $^{147}\text{Sm}(d,p)^{148}\text{Sm}$ angular distributions to the 3^- state, $l=2$ strength seems to be quite likely. The curve results from a $2d_{3/2}$ DWBA pickup calculation. Only statistical errors are included.

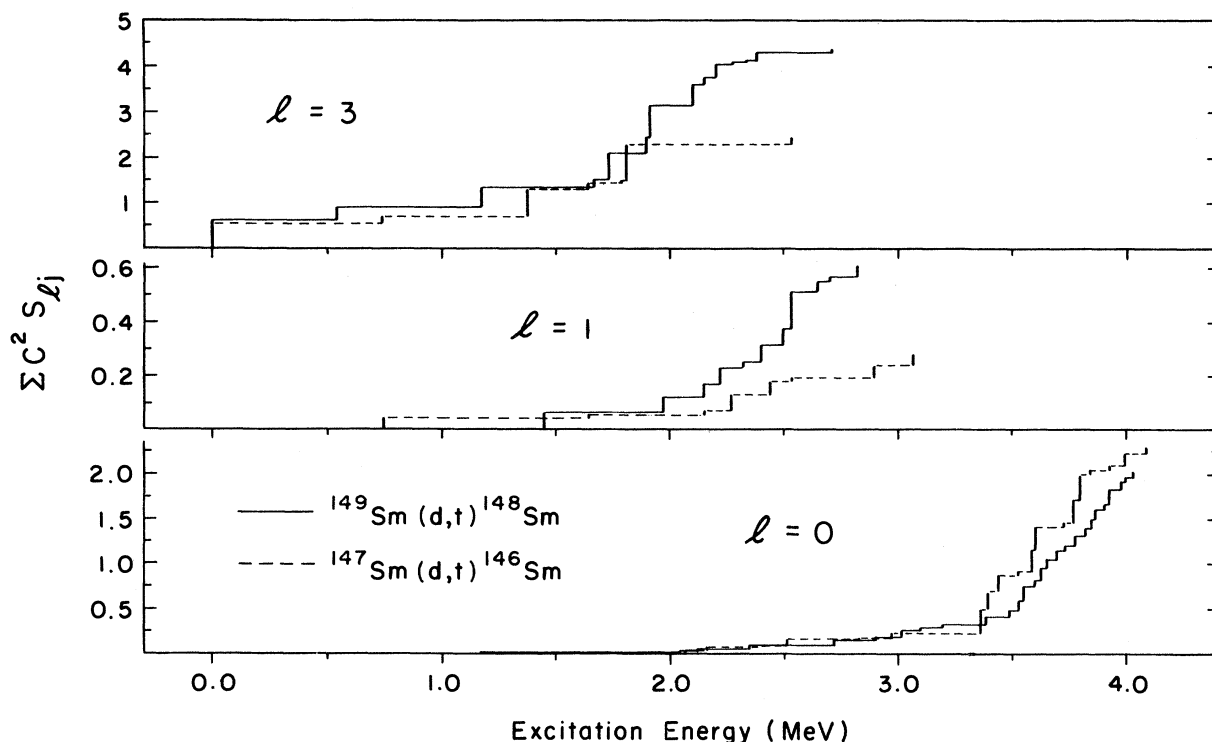


FIG. 22. Sum of spectroscopic factors as function of excitation energy for the (d, t) reactions on ^{147}Sm and ^{148}Sm .

level No. 5. The two states at 2.206 MeV (No. 30) and 2.220 MeV (No. 32) have been reported in each of two independent (p, t) studies.^{10, 29} The 2.206 MeV level was identified as $J^\pi = 0^+$ and the 2.220 MeV level was tentatively assigned $J^\pi = 0^+$ with a speculation that the two might be one level. In fact both levels have been observed in the present study—the spin limits are compatible with $J^\pi = 0^+$ for the 2.206 MeV level but not for the state at 2.220 MeV. In all other J^π limits extracted no discrepancy between the present data and former spin and parity assignments is found.

The level at 1.162 MeV (No. 2) is weakly excited

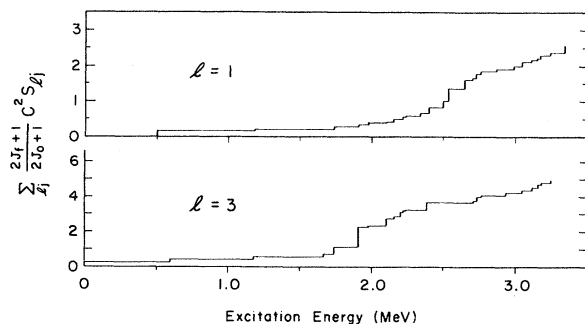


FIG. 23. Sum of spectroscopic factors as function of excitation energy for the $^{147}\text{Sm}(d, p)$ reaction.

in all reactions induced by charged particles but shows up strongly in deuteron scattering.⁴⁵ This indicates the collective nature of this 3^- state of the octupole band. The 1^- state of this band [1.465 MeV (No. 7)] does not show up in any neutron transfer reaction. The same is true for the 1.434 MeV state (No. 5) which is not excited in scattering experiments either and therefore is probably of unnatural parity.

In the light of the shape transition the isotopes of Sm undergo with increasing neutron number the following observation is of interest: In ^{146}Sm the supposed 2^+ state of the quasi γ band (1.648 MeV)³⁰ is rather strongly excited via the (d, t) reaction but the same 2^+ state proposed to be at 1.432 excitation energy³⁰ in ^{148}Sm is not observed in this investigation. On the other hand, the 2^+ state of the quasi β band³⁰ shows up clearly in ^{148}Sm via both reactions (1.666 MeV, No. 10), but seems to be less populated in ^{146}Sm (2.157 MeV, No. 15).

VII. SUMMARY

The reactions $^{147, 149}\text{Sm}(d, t)$ and $^{147}\text{Sm}(d, p)$ have been investigated with the intention of identifying the single particle/single hole characteristics of the states in the residual even-even Sm nuclei: A phenomenological model is introduced to parallel

the pairing vibrational terminology used to describe the population of some residual states of the same nuclei in two-neutron transfer studies. Although the high ($\frac{7}{2}$) spin of the odd-mass Sm targets limits the quantity of spectroscopic information that can be extracted from these single neutron transfer reactions, it has been possible to evolve a coherent picture of single particle and hole strengths in these interesting shape transitional nuclei. The low lying levels (below 1.9 MeV excitation energy) of both ^{146}Sm and ^{148}Sm show dominant quasihole state character. Quasi-particle states populated in ^{148}Sm via the (d, p) reaction predominate in the excitation energy range of 1.9 to 3.3 MeV. Presumably this observation is even more pronounced for the final nucleus ^{146}Sm , indicated by an obvious low yield in this excitation energy region in the (d, t) reaction.

The quasihole states in both (d, t) reactions are due to a pickup from the $2f_{7/2}$ and $3p_{3/2}$ orbitals of the $82 < N \leq 126$ shell for the low lying states and at higher excitation energies (centered around 3.6 MeV) are nearly exclusively due to a $3s_{1/2}$ pickup from the $50 < N \leq 82$ shell.

Whereas in the $^{147}\text{Sm}(d, t)$ reaction hardly any $l=3$ transfer beyond the gap energy is observed, 40% of this strength shows up in the $^{149}\text{Sm}(d, t)$ reaction above the breaking energy for a neutron pair.

$^{147}\text{Sm}(d, p)$ strength has been observed to be al-

most exclusively $l=1$ and $l=3$ strength, indicating a stripping to the $2f_{7/2}$ and $3p_{3/2}$ subshells.

The lack of higher l -transfer yield is not fully understood. However, it may be attributed to some combination of the following factors: (1) strong fragmentation, (2) the domination of mixed l transitions by the intrinsically stronger low l contributions, and (3) multistep processes. Especially since the Sm isotopes are known to undergo shape transitions and show shape coexistence effects these multistep processes seem to be likely. The fact that some $l=5$ strength has tentatively been observed ($C^2S_{ij}=1.9$) in the $^{147}\text{Sm}(d, t)$ reaction but not in the $^{149}\text{Sm}(d, t)$ study gives a hint in this direction because shape coexistence is most strongly observed in ^{150}Sm and ^{152}Sm and decreases to lower and higher mass.

Phenomenologically our results are in quantitative agreement with two-nucleon transfer data for the low lying levels of ^{146}Sm and ^{148}Sm .

ACKNOWLEDGMENTS

We are very grateful to Dr. R. M. Drisko for discussions on parts of this paper. We would like to thank Mrs. A. Trent for developing and scanning our plates. We appreciate the hospitality and assistance of Dr. J. R. Erskine, Ms. E. Sutter, and Ms. L. Gritter in using the Argonne automatic plate scanner.

*Work supported by National Science Foundation.

¹M. E. Bunker and C. W. Reich, *Rev. Mod. Phys.* **43**, 348 (1971); B. Arad and G. Ben-David, *ibid.* **45**, 230 (1973), and references therein.

²*Nuclear Level Schemes A=45 through A=257 from Nuclear Data Sheets*, edited by D. J. Horen *et al.* (Academic, New York, 1973).

³W. Gelletly and W. R. Kane, *Phys. Rev. C* **6**, 1113 (1972).

⁴O. J. Buss and R. K. Smither, *Phys. Rev. C* **2**, 1513 (1970).

⁵M. P. Avotina, E. P. Grigoriev, V. O. Sergeev, and A. V. Zolotavin, *Phys. Lett.* **19**, 310 (1965).

⁶W. Oyle, S. Wahlborn, R. Piepenbring, and S. Frederiksson, *Rev. Mod. Phys.* **43**, 424 (1971), and references therein.

⁷R. J. Ascutto and J. S. Vaagen, in *Proceedings of the International Conference on Reactions between Complex Nuclei, Nashville, Tennessee, 10-14 June, 1974*, edited by R. L. Robinson, F. K. McGowan, J. B. Ball, and J. H. Hamilton (North-Holland, Amsterdam/American Elsevier, New York, 1974), Vol. 2, p. 257, Ref. 2 therein.

⁸A. Friedeman and K. Katori, *Phys. Rev. Lett.* **30**, 102 (1973).

⁹J. V. Maher, J. J. Kolata, and R. W. Miller, *Phys. Rev. C* **6**, 358 (1972).

¹⁰W. Oelert, G. Lindstroem, and V. Riech, *Nucl. Phys.*

A233, 237 (1974), and references therein.

¹¹J. R. Erskine and R. H. Vonderohe, *Nucl. Instrum. Methods*, **181**, 221 (1970).

¹²J. R. Comfort, ANL Physics Division Informal Report No. PHY-1970 B, 1970 (unpublished); P. Sprink and J. R. Erskine, ANL Physics Division Informal Report No. PHY-1965 B, 1965 (unpublished).

¹³P. D. Kunz, Univ. of Colorado, Boulder (unpublished).

¹⁴E. R. Flynn, D. D. Armstrong, J. G. Beery, and A. G. Blair, *Phys. Rev.* **182**, 1113 (1969).

¹⁵F. D. Becchetti and G. W. Greenlees, Univ. of Minnesota Annual Report, 1969 (unpublished).

¹⁶F. D. Becchetti and G. W. Greenlees, *Phys. Rev.* **182**, 1190 (1969).

¹⁷C. Pegel, Ph.D. thesis, Univ. of Hamburg, 1973 (unpublished).

¹⁸J. D. Childs, W. W. Daehnick, and M. J. Spisak, *Phys. Rev. C* **10**, 217 (1974).

¹⁹C. A. Wiedner, A. Heusler, J. Solf, and J. P. Wurm, *Nucl. Phys.* **A103**, 433 (1967).

²⁰R. H. Bassel, *Phys. Rev.* **149**, 791 (1966).

²¹R. H. Fulmer, A. L. McCarthy, and B. L. Cohen, *Phys. Rev.* **128**, 1302 (1962).

²²R. K. Jolly and E. Kashy, *Phys. Rev. C* **4**, 887 (1971).

²³R. K. Jolly and E. Kashy, *Phys. Rev. C* **4**, 1398 (1971).

²⁴A. Chaumeaux, G. Bruge, H. Faraggi, and J. Picard, *Nucl. Phys.* **A164**, 176 (1971).

²⁵J. L. Foster, Jr., O. Dietzsch, and D. Spalding, *Nucl.*

- Phys. A169, 187 (1971).
- ²⁶K. Yagi, *J. Phys. Soc. Jpn.* 24, 559 (1968).
- ²⁷K. Yagi, T. Ishimatsu, Y. Ishizaki, and Y. Saji, *Nucl. Phys.* A121, 161 (1968).
- ²⁸J. H. Bjerregaard, O. Hansen, and O. Nathan, *Nucl. Phys.* 86, 145 (1966).
- ²⁹P. Debenham and N. M. Hintz, *Nucl. Phys.* A195, 385 (1972).
- ³⁰M. Sakai, *Nucl. Data* A8, 334 (1970).
- ³¹R. Kenefick and R. K. Sheline, *Phys. Rev.* 133, B25 (1964).
- ³²J. J. Kolata and J. V. Maher, *Phys. Rev. C* 8, 285 (1973).
- ³³J. V. Maher, G. H. Wedberg, J. J. Kolata, J. C. Peng, and J. L. Ricci, *Phys. Rev. C* 8, 2390 (1973).
- ³⁴M. Jaskola, P. O. Tjøm, and B. Elbek, *Nucl. Phys.* A133, 65 (1969).
- ³⁵S. Gales, L. Lessard, and J. L. Foster, Jr., *Nucl. Phys.* A202, 535 (1972).
- ³⁶W. Booth, S. Wilson, and S. S. Ipson, *Nucl. Phys.* A229, 61 (1974).
- ³⁷R. J. Ascutto, C. H. King, and L. J. McVay, *Phys. Rev. Lett.* 29, 1106 (1972).
- ³⁸R. D. Gadsby, D. G. Burke, and J. C. Waddington, *Can. J. Phys.* 51, 203 (1973).
- ³⁹O. Nathan, in *Proceedings of the International Symposium on Nuclear Structure, Dubna, 1968* (International Atomic Energy Agency, Vienna, Austria, 1969); A. Bohr, *ibid.*, p. 179.
- ⁴⁰G. Igo, P. D. Barnes, and E. R. Flynn, *Ann. Phys. (N.Y.)* 66, 60 (1971).
- ⁴¹R. A. Broglia, O. Hansen, and C. Riedel, *Advan. Nucl. Phys.* 6, 287 (1973).
- ⁴²K. Yagi, Y. Aoki, and K. Sato, *Nucl. Phys.* A149, 45 (1970).
- ⁴³T. J. Mulligan, E. R. Flynn, O. Hansen, R. F. Casten, and R. K. Sheline, *Phys. Rev. C* 6, 1802 (1972).
- ⁴⁴C. M. Cheng, J. V. Maher, W. Oelert, D. A. Sink, and M. J. Spisak, *Bull. Am. Phys. Soc.* 19, 1011 (1975).
- ⁴⁵E. Veje, B. Elbek, B. Herskind, and M. C. Olesen, *Nucl. Phys.* A109, 489 (1968).